nature COMMUNICATIONS

ARTICLE

Received 15 Oct 2013 | Accepted 20 Mar 2014 | Published 17 Apr 2014

DOI: 10.1038/ncomms4708 OPEN

Unc5C and DCC act downstream of Ctip2 and Satb2 and contribute to corpus callosum formation

Swathi Srivatsa[1,2,*], Srinivas Parthasarathy[1,2,*], Olga Britanova[1,3], Ingo Bormuth[1], Amber-Lee Donahoo[4], Susan L. Ackerman[5], Linda J. Richards[4] & Victor Tarabykin[1]

The pyramidal neurons of the mammalian neocortex form two major types of long-range connections—corticocortical and cortico-subcortical. The transcription factors Satb2 and Ctip2 are critical regulators of neuronal cell fate that control interhemispheric versus corticofugal connections respectively. Here, we investigate the axon guidance molecules downstream of Satb2 and Ctip2 that establish these connections. We show that the expression of two Netrin1 receptors- *DCC* and *Unc5C* is under direct negative regulation by Satb2 and Ctip2, respectively. Further, we show that the Netrin1–Unc5C/DCC interaction is involved in controlling the interhemispherical projection in a subset of early born, deep layer callosal neurons.

[1] Institute for Cell and Neurobiology, Center for Anatomy, Charité- Universitätsmedizin Berlin, Virchowweg 6, 10117 Berlin, Germany. [2] Max Planck Institute for Experimental Medicine, Hermann-Rein-Strasse. 3, 37075 Goettingen, Germany. [3] Shemyakin and Ovchinnikov Institute for Bioorganic Chemistry RAS, Miklukho-Maklaya, Moscow 117997, Russia. [4] Queensland Brain Institute, School of Biomedical Sciences, The University of Queensland, Brisbane, Queensland 4072, Australia. [5] Howard Hughes Medical Institute and The Jackson Laboratory, 600 Main Street, Bar Harbor, Maine 04609, USA. * These authors contributed equally to this work. Correspondence and requests for materials should be addressed to V.T. (email: Victor.tarabykin@charite.de).

The neocortex is the neural substrate of our higher cognitive abilities, helping us perceive, understand and react to the environment. Such a formidable task is made possible by the staggering number of neurons that constitute the neocortex forming functional connections both within the neocortex as well as with other targets in the central nervous system. Such long-range connections are crucial for brain function and the efficient integration and exchange of information.

The long-range connections of the neocortex can be broadly classified into two types: interhemispheric connections versus corticofugal connections. While most deeper layer neurons (layer V–VI) make corticofugal connections, upper layer neurons (II–III) and some neurons of layer V connect the two hemispheres of the telencephalon. Although both laterally and medially projecting layer V neurons are born at the same time, laterally projecting neurons extend an axon ~2 days before the medially projecting layer V neurons[1]. The corpus callosum (CC) is the primary conduit for transmission and coordination of information between neurons of the two cerebral hemispheres. Evolutionarily, the mammalian neocortex has undergone a substantial increase in the proportion of upper layer neurons suggesting that the corresponding increase in corticocortical connections is one of the primary reasons for the increase in the cognitive abilities witnessed through mammalian evolution[2–4]. It is hence no surprise that malformation or agenesis of the CC can lead to severe cognitive disabilities[5].

Although it has been well established that neurons form connections through specific and predetermined trajectories in the brain in response to several guidance cues present in the environment, our understanding of how cellular identities govern the appropriate responses of axons to these guidance cues and hence direct the establishment of these precise connections remains incomplete, more so for forebrain structures such as the neocortex[1].

Two genes, *Satb2 and Ctip2,* have been shown in recent years to orchestrate important and mutually exclusive genetic programs that establish corticocortical versus corticofugal connections, respectively[6–8]. While Satb2, a matrix attachment region (MAR) interacting protein has been shown to be indispensable for the formation of the CC, Ctip2 on the other hand is required for the fasciculation and pathfinding of subcortically projecting neurons[6,9].

Interestingly, the deletion of *Satb2* in the cortex leads to an ectopic upregulation of *Ctip2* in upper layer neurons, with a corresponding misrouting of callosally projecting neurons to subcortical targets[7,8]. Thus, in normal development, *Satb2* overrides the *Ctip2* driven molecular pathway in order to establish interhemispheric projections versus corticofugal projections.

In this study, we investigated the downstream molecular events in this Satb2—*Ctip2* interaction. We identified that two Netrin1 receptors, *DCC* and *Unc5C*, are controlled by both Satb2 and Ctip2. Unc5C and DCC play important roles in guiding commissural axons in various systems[10–15]. DCC can mediate an attractive response to a Netrin1 source, while Unc5C, in a DCC-dependent or -independent manner, has been shown to mediate a repulsive response[11,12,15–18].

Here, we show that Ctip2 and Satb2 negatively regulate *Unc5C* and *DCC*, respectively. This in turn mediates a differential response of neocortical axons to Netrin1. High levels of *Unc5C* expression, and low levels of *DCC* expression, instruct neurons to project through the CC, since in the absence of either *Unc5C* or *Netrin1*, callosal axons misproject to subcortical targets, mimicking the effect of *Satb2* mutation. In contrast, inactivation of *Ctip2* and *DCC*, or the restoration of *Unc5C* in *Satb2* mutants, can partially restore CC formation. Thus, a dynamic regulation of *Unc5C* and *DCC* by Ctip2 and Satb2 paves the way for the appropriate formation of interhemispheric and corticofugal neocortical projections, at least for a subset of deep layer callosal neurons.

Results

***Unc5C* expression requires Satb2**. In order to identify molecules downstream of Satb2 that control CC formation, we investigated changes in the expression of a variety of axon guidance molecules in the Satb2$^{-/-}$ mutants. We assumed that such molecules should be downregulated in *Satb2*-mutant cortex and that their expression should be confined to callosal neurons (Satb2 positive), while being excluded from corticofugal neurons (Ctip2 positive). Among others tested, the expression of the Netrin1 receptor, Unc5C, satisfied these two criteria. *Unc5C* expression was previously shown to be downregulated in *Satb2*$^{-/-}$ mutants[7,19]. Here, *in situ* hybridization against the *Unc5C* messenger RNA (mRNA) showed a complete loss of *Unc5C* from the *Satb2*$^{-/-}$ cortical plate, with only expression in the subplate remaining (Fig. 1a). Further, *Unc5C* has a very dynamic expression pattern during cortical development. At E14.5 *Unc5C* is predominantly expressed in the subplate. At E18.5, the expression of *Unc5C* in the cortical plate reaches a very high level and demonstrates a high-lateral to low-medial gradient (Fig. 1a,b).

To test whether ectopic and premature expression of *Satb2* can induce *Unc5C* expression, we performed *in utero* electroporation of *Satb2* and *Ski* expressing plasmids into the lateral ventricle at E12.5 and analysed the brains at E14.5. Satb2 requires Ski as a cofactor for recruiting chromatin remodelling complexes and thus silencing its targets[20]. This experiment induced ectopic expression of *Unc5C* in the cells electroporated with *Satb2* compared with a control construct (Fig. 1b).

To test our hypothesis that *Unc5C* is expressed by callosally projecting Satb2-positive cells and absent in Ctip2-positive cells, we combined *in situ* hybridization (ISH) using a probe against *Unc5C* and immunohistochemistry (IHC) using antibodies against Satb2 and Ctip2. *Unc5C* mRNA is expressed predominantly in upper layers and weakly in deeper layers. Since combining ISH and IHC requires the omission of proteinase K from the protocol, a physical limitation to the extent of probe penetration is an unavoidable drawback. Thus, even though in conventional ISH, *Unc5C* expression is seen in both upper and deeper layers, with FISH the expression was detected in separate experiments. We observed that *Unc5C* and Ctip2 were not expressed in the same cells in most cases whereas *Unc5C* and Satb2 were usually co-expressed. Even in layer V, *Unc5C* and Satb2 were co-expressed but neither was expressed in Ctip2-positive cells (Fig. 1c). This indicates that Satb2 could also repress *Ctip2* in deep layer neurons, in addition to the previously reported repression in upper layer neurons (Supplementary Fig. 1A,B).

Unc5C* is directly repressed by *Ctip2. Since *Unc5C* and *Ctip2* are not co-expressed, we hypothesized that *Unc5C* expression could be negatively regulated by Ctip2. To investigate this, we examined whether Unc5C expression would be restored in *Satb2*$^{-/-}$; *Ctip2*$^{-/-}$ double mutants. We observed an increase of Unc5C expression in *Satb2*$^{-/-}$; *Ctip2*$^{-/-}$ mutant cortex as compared with *Satb2*$^{-/-}$ mutants. In *Ctip2*$^{-/-}$ single mutants we did not detect significant changes in Unc5C expression compared with controls (Fig. 2a). In all further experiments, wild type, *Satb2* heterozygous, *Ctip2* heterozygous and *Satb2/Ctip2* compound heterozygous embryos have all been referred to interchangeably as controls.

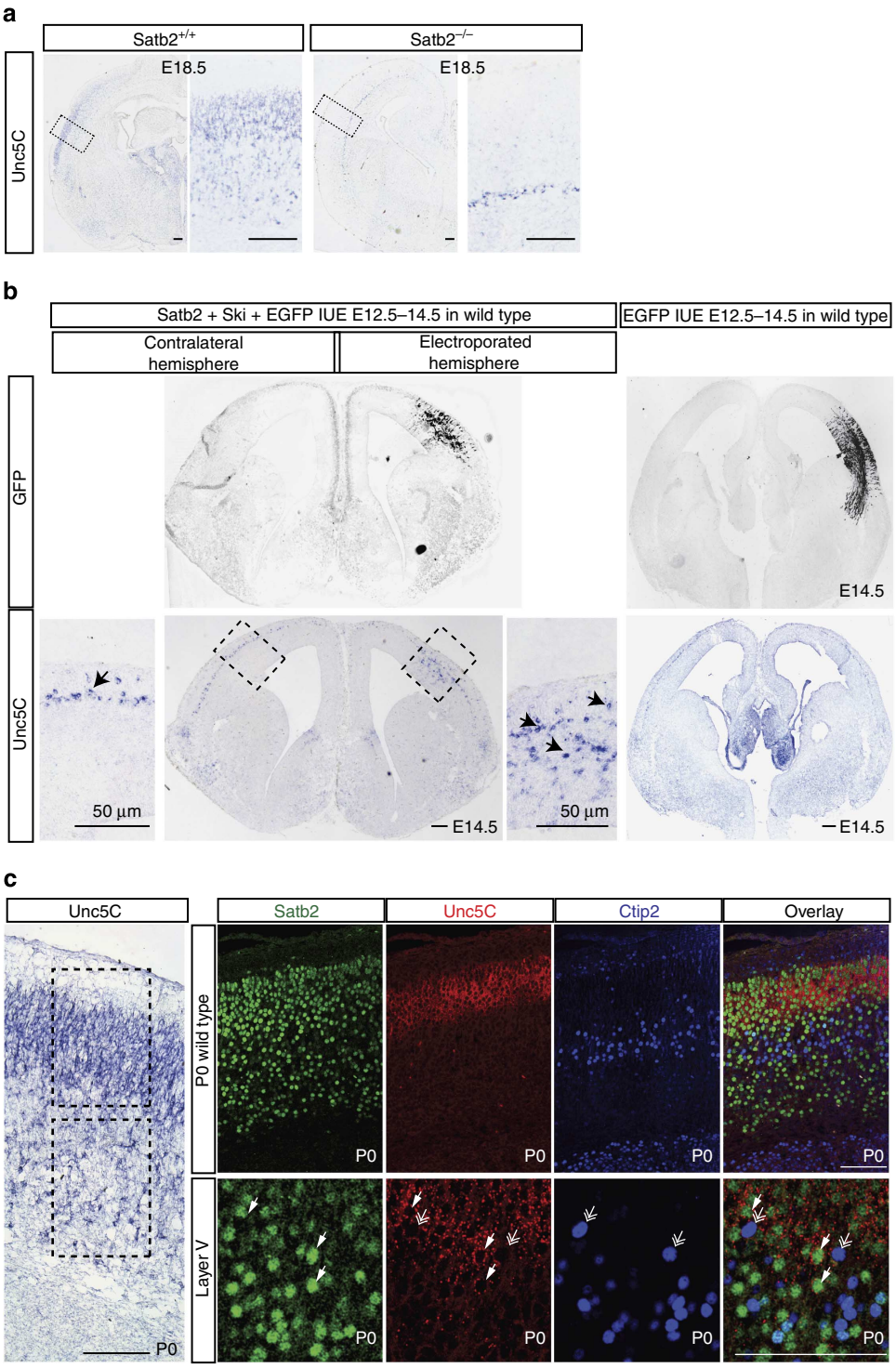

Figure 1 | Unc5C is expressed by callosally projecting Satb2-positive neurons and Satb2 regulates *Unc5C* expression. (**a**) *Unc5C* mRNA expression in wild-type and *Satb2*$^{-/-}$-mutant mice at E18.5. In sections of *Satb2*$^{-/-}$-mutant brains, *Unc5C* continues to be expressed in only the subplate, but is absent in other cortical layers. (**b**) *Unc5C* expression in E14.5 wild-type embryos in cells that were electroporated at E12.5 with *Satb2/Ski/EGFP* or *EGFP* control. GFP IHC depicts the region electroporated. *Unc5C in situ* hybridization shows additional ectopic expression of *Unc5C* within cells electroporated with *Satb2/Ski* apart from the expression in the subplate seen in the contralateral hemisphere or in the control electroporation. (**c**) *Unc5C* mRNA expression with respect to Satb2 and Ctip2-expressing cells through immunofluorescence/fluorescence ISH in P0 wild-type cortex. High magnification of P0 wild-type cortex shows that *Unc5C* is expressed primarily in the upper layers but also in a subset of cells in the deep layers—layer V (boxed regions) *Unc5C* mRNA expression coincides with the expression of Satb2 and is excluded from Ctip2-expressing cells. Layer V expression of *Unc5C* is restricted to cells expressing Satb2 (arrows) and absent in Ctip2-positive cells (double arrowheads). Scale bar, 100 µm, unless specified differently in the figure.

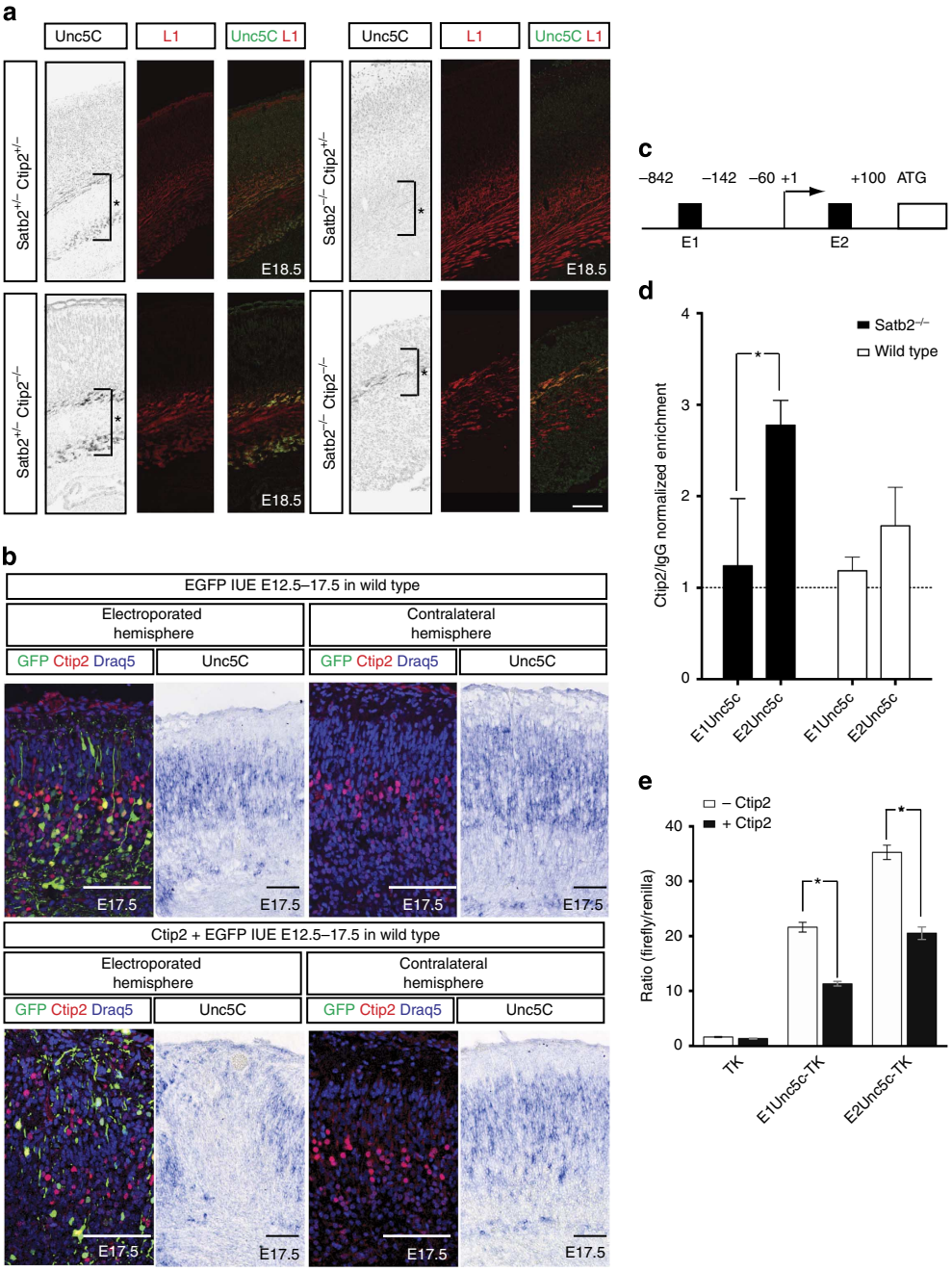

Figure 2 | Ctip2 directly represses *Unc5C* expression. (**a**) Immunohistochemical staining against Unc5C and L1. Unc5C expression is absent in *Satb2*$^{-/-}$ brains when compared with wild-type and *Ctip2*$^{-/-}$ brains. The expression of Unc5C is restored in *Satb2*$^{-/-}$;*Ctip2*$^{-/-}$ double-mutant brains. (**b**) *Unc5C* expression in E17.5 wild-type embryos in cells electroporated at E12.5 with *Ctip2/EGFP* or *EGFP* control within the electroporated as well as contralateral hemisphere. Subsequent section stained for GFP, Ctip2, Draq5 (a nuclear marker) IHC. *Unc5C* mRNA expression is lost in the region electroporated with *Ctip2* when compared with either the control electroporation or the corresponding region in the contralateral hemisphere. (**c**) Scheme showing the two regions in the *Unc5C* promoter where Ctip2 was predicted to bind. (**d**) ChIP from P0 cortex of wild-type and *Satb2*$^{-/-}$ mutants show that Ctip2 binds to the *Unc5C* promoter region. 2.78 ± 0.2722-fold enrichment for E2 compared with 1.23 ± 0.73 for E1 in *Satb2*$^{-/-}$, $n = 3$, *P*-value = 0.027 (Student's *t*-test) and 1.67 ± 0.42-fold enrichment for E2 compared with 1.18 ± 0.14 for E1 in wild type $n = 4$, NS. (**e**) Luciferase assay to demonstrate that Ctip2 binds to *Unc5C* genomic region and represses its expression. In the presence of full-length Ctip2, 1.9- and 1.7-fold decrease in luminescence ratio was observed in case of E1 and E2, respectively. E1 and E2 being two putative Ctip2-binding sites. All *P-values were ≤0.05, Student's *t*-test $n = 3$. Scale bar, 100 μm.

This result indicated that in *Satb2*$^{-/-}$ mutants, the down-regulation of *Unc5C* could be the result of the ectopic upregulation of *Ctip2*. To test this hypothesis, we overexpressed *Ctip2* in the cortex. An *EGFP*-expression plasmid was electroporated either alone or with the *Ctip2* expression plasmid in wild-type E12.5 embryos and the brains were harvested at E17.5. Ctip2 expression was validated in HEK293T cells (Supplementary Fig. 2A) and a confocal maximum Z-projection image for the electroporated region also confirmed the expression of Ctip2 in a large population of cortical cells (Supplementary Fig. 2B).

Subsequent sections were labelled with a probe against *Unc5C* mRNA. A decrease in *Unc5C* expression was observed in *Ctip2* overexpressing cells within the electroporated cortical region, as compared with the contralateral hemisphere ($n=3$) or *EGFP*-alone electroporated brains ($n=2$, Fig. 2b).

Next, we investigated whether Ctip2 directly represses *Unc5C* expression. An *in silico* search revealed two putative Ctip2-binding sites in the *Unc5C* promoter, that we designated E1 and E2 (-842 to -142 and -60 to $+100$) upstream of the transcription-initiation site (Fig. 2c). Chromatin immunoprecipitation (ChIP) from wild-type and *Satb2*$^{-/-}$ cortices followed by quantitative real time polymerase chain reaction, showed that Ctip2 binds strongly to the E2 but not the E1 *Unc5C* promoter region. *Satb2*$^{-/-}$ cortices were used as a means of enriching for Ctip2-positive cells in the cortex (Fig. 2d, 2.78 ± 0.2722-fold enrichment for E2 compared with 1.23 ± 0.73 for E1 in Satb2$^{-/-}$, $n=3$, P-value $=0.027$ (Student's t-test) and 1.67 ± 0.42-fold enrichment for E2 compared with 1.18 ± 0.14 for E1 in wild type, $n=4$, NS).

To confirm this result we performed an *in vitro* luciferase assay. In these experiments, the same two *Unc5C* upstream genomic regions E1 and E2 were inserted into a plasmid encoding the luciferase gene and transfected into cells with a plasmid encoding *Ctip2*. We observed a decrease in the activity of the *Unc5C* promoter by $\sim$1.9-fold and 1.7-fold, in the case of E1 and E2 respectively, when *Ctip2* was co-transfected (Fig. 2e, both P-values <0.05, Student's t-test, $n=3$). These results indicate that Ctip2 can directly repress *Unc5C* transcription.

Partial restoration of the CC in *Satb2*$^{-/-}$;*Ctip2*$^{-/-}$ mutants. Others and we have previously shown that the deletion of *Satb2* results in the ectopic upregulation of *Ctip2* and misprojection of callosal axons laterally[7,8]. Since *Satb2* and *Ctip2* regulate divergent genetic programs, that control the formation of interhemispheric versus corticofugal projections, we investigated whether downregulating *Ctip2* in the *Satb2*$^{-/-}$ cortex could restore CC formation. We analysed *Satb2*$^{-/-}$;*Ctip2*$^{-/-}$ double-mutant animals for the presence of the CC. To visualize callosal axons, we introduced a plasmid coding for *Venus-green fluorescent protein (GFP)* in neocortical cells by *in utero* electroporation at E12.5 and harvested the brains at E18.5. We found that while in *Satb2*$^{-/-}$ animals, no cortical axons approached or even turned towards the dorsal midline, in *Satb2*$^{-/-}$;*Ctip2*$^{-/-}$ compound mutants, GFP-positive axons approached, crossed the midline and invaded the contralateral cortex. It is noteworthy though that the number of crossing axons that projected into the contralateral hemisphere were fewer when compared with that seen in wild-type and *Ctip2*$^{-/-}$ littermates (Fig. 3a). The results were quantified by measuring the fluorescent area of the fibres projecting medially with respect to the fluorescent area of the electroporated region in the cortex (Supplementary Fig. 3). To rule out the possibility of axonal outgrowth defects in *Satb2*-negative neurons as a cause for the lack of extension of the axons contralaterally, we performed an *in vitro* axon outgrowth assay, but did not observe an axonal outgrowth deficit in *Satb2*-deficient neurons (Supplementary Fig. 4). Another possibility was that the axons were indirectly affected due to changes in the formation of midline guidepost structures in the *Satb2* mutant and *Satb2*$^{-/-}$;*Ctip2*$^{-/-}$ double mutants. To examine this, we stained for midline guidepost cells with calretinin and glial fibrillary acidic protein (Supplementary Fig. 5). We did not detect any differences in the size or morphology of midline structures between the different genotypes suggesting that *Satb2*-deficient neurons are defective in axonal targeting and not outgrowth or midline crossing.

Restoring *Unc5C* expression in Satb2$^{-/-}$ partially rescues the CC. Since the *Satb2*$^{-/-}$;*Ctip2*$^{-/-}$ double mutants showed a partial rescue of callosal crossing fibres and an increased Unc5C expression compared with single mutants, we tested whether we could rescue callosal fibres in *Satb2*$^{-/-}$ mutants by overexpressing *Unc5C*. An *Unc5C*-expressing plasmid was co-expressed with *Venus-GFP* at E12.5 and compared with *Venus-GFP* expression alone in *Satb2*$^{-/-}$ as well as control brains. We observed that axons of the *Unc5C* electroporated neurons in the *Satb2*$^{-/-}$ cortex extended medially, and crossed the midline ($n=3$). This rescue was again only partial as fewer axons crossed the midline compared with that in the control animals (Fig. 3b). Electroporation of only *Venus-GFP* in *Satb2*$^{-/-}$ embryos served as a negative control where no callosally extending fibres were observed (Fig. 3a). The extent of callosal midline crossing with electroporation of *Unc5C* was comparable with the partial rescue obtained in *Satb2*$^{-/-}$;*Ctip2*$^{-/-}$ double mutants at E12.5 (Fig. 3a,b, Supplementary Fig. 3). Interestingly, *Unc5C* could not restore the callosal fibres when overexpressed at E14.5 (Supplementary Fig. 6A).

Neocortical callosal axons are repelled by Netrin1. Unc5C has been shown to be a receptor for the secreted ligand Netrin1, mediating long range repulsive signalling[12,16]. Since we observed that the formation of callosal projections depended upon the presence of *Unc5C* expression, we tested whether these Unc5C-positive callosally projecting neurons were also responsive to Netrin1. To test this, we devised a slice culture system where wild-type embryos were co-electroporated with either *Unc5C* and *EGFP* (Fig. 4a) or only *EGFP* (Fig. 4b) at E12.5 and harvested at E16.5. Slices prepared from these brains were cultured for 3 days *in vitro* and Netrin1-soaked agarose beads were placed in the midline at the position where callosal fibres cross. If the *Unc5C*-positive callosal axons were responsive to the repulsive Netrin1 signal, then they would be prevented from crossing the midline upon encountering the ligand in their trajectory. When *Unc5C*-positive fibres encountered Netrin1-soaked beads in the midline, they were repelled and did not cross the midline. Instead they misprojected ventrally or dorsally within the ipsilateral hemisphere showing an avoidance behaviour towards the beads. Conversely, when these *Unc5C*-positive axon fibres encountered bovine serum albumin (BSA)-soaked beads, they were unaffected and continued in their trajectory, crossing the midline and entering the contralateral hemisphere (Fig. 4a). This experiment indicated that *Unc5C*-expressing cortical neurons are indeed repelled by a Netrin1 source. By expressing only *EGFP* in cortical neurons, we tested our hypothesis that if callosal fibres express *Unc5C* endogenously, then they would also be repelled from a Netrin1 source. Again, these fibres failed to cross the midline upon encountering Netrin1, whereas BSA-coated beads posed no hindrance to the midline crossing (Fig. 4b).

Satb2-positive axons misproject in Netrin1 and Unc5C mutants. Since *Unc5C* is expressed in Satb2-positive neurons (Fig. 1c), and their axons are repelled by Netrin1 *in vitro* (Fig. 4), we asked whether *Netrin1* deletion would have any effect on axons of these neurons *in vivo*. In the developing telencephalon, *Netrin1* is expressed in the basal ganglia and ventral midline[14,21]. We reasoned that the source of Netrin1 in the basal ganglia might normally repel the axons of *Satb2*-positive/*Unc5C*-positive neurons from the internal capsule. We hypothesized that Satb2-positive neurons would misproject to subcortical targets in *Netrin1*-deficient brains. To test this hypothesis, we placed crystals of the lipophilic tracer DiI at the cerebral peduncle of E17.5 *Netrin1* hypomorph and wild-type brains to retrogradely

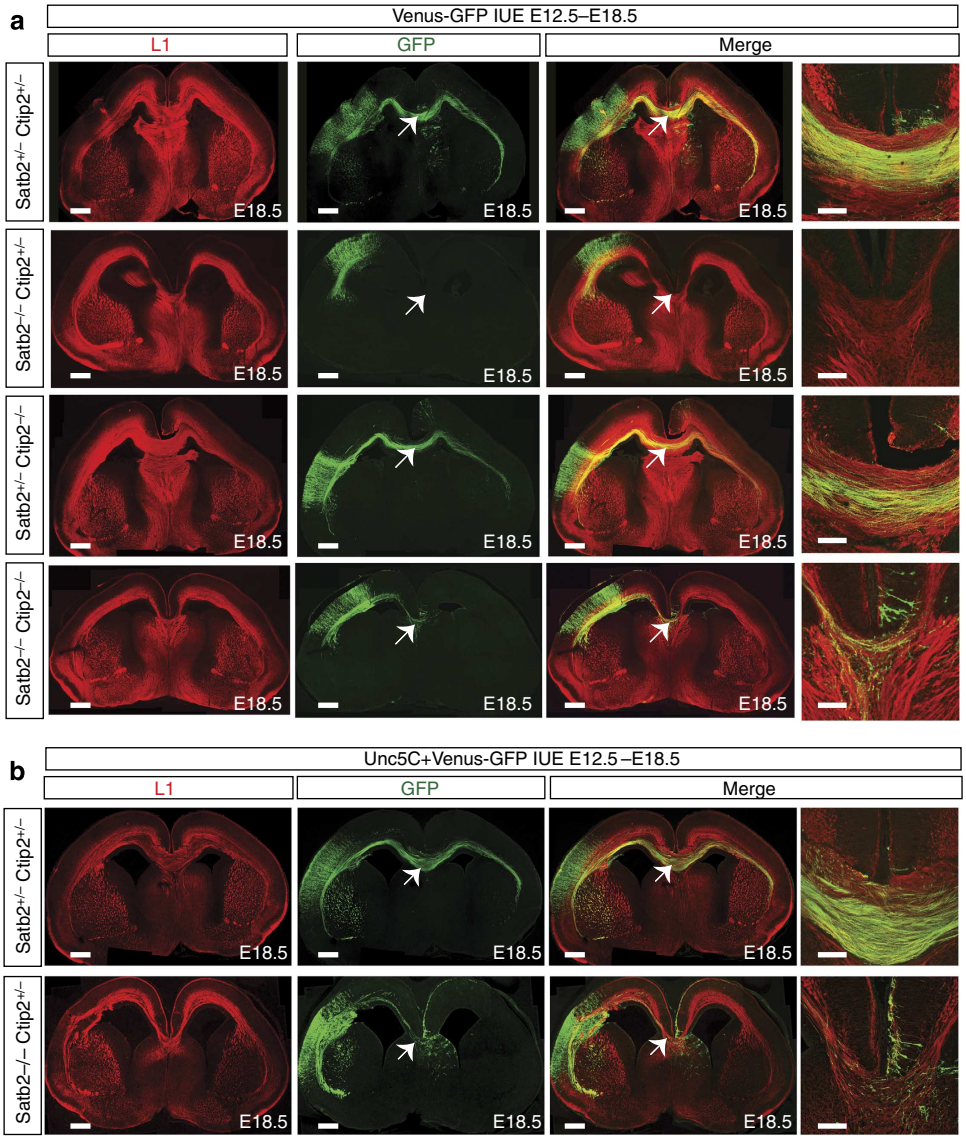

Figure 3 | The CC is partially restored in *Satb2*$^{-/-}$ mutants by deleting *Ctip2* or by overexpressing *Unc5C*. (**a**) Images with higher magnification of the midline show a series of experiments, wherein *Venus-GFP* was electroporated into the developing cortex at E12.5 and the brains harvested and analysed at E18.5. Electroporation of *Venus-GFP* shows a normal CC in wild-type and *Ctip2*$^{-/-}$ embryos. *Satb2*$^{-/-}$-mutant brains clearly demonstrate a complete absence of callosal fibres, wherein no fibres could be seen approaching the midline. Partial rescue of the CC could be seen in *Satb2*$^{-/-}$; *Ctip2*$^{-/-}$ compound mutants. Fibres manage to reach and cross the midline (arrows). The sections have been subjected to immunohistochemical staining for the neural cell adhesion molecule L1 and for GFP. (**b**) Images show the result of *Unc5C/EGFP* overexpression in wild-type and *Satb2*$^{-/-}$-mutant cortex. Overexpression of *Unc5C* in *Satb2*$^{-/-}$ partially restores the CC where axons of electroporated neurons reach and cross the midline (arrow). Normally projecting callosal axons were observed in the control cortex. Scale bar, 450 μm for low-magnification images and 100 μm for high-magnification images.

trace the neurons that project subcortically. After staining these sections with an antibody against Satb2, we counted the proportion of DiI-positive retrogradely labelled neurons that were also Satb2 positive (Fig. 5a). We observed that the proportion of Satb2-positive DiI-labelled cells representing the proportion of Satb2-positive, subcortically projecting neurons, almost doubled in *Netrin1* hypomorph brains compared with their wild-type littermates (Fig. 5b, 15.36% in wild type compared with 27.33% in *Netrin1* hypomorph, P-value = 0.011, Student's t-test, $n = 3$).

We also tested whether *Unc5C* ablation in neocortical neurons would cause a similar effect. In contrast to the acallosal *Netrin1* hypomorph, *Unc5C* mutants display callosal fibres crossing the midline. We therefore tested whether some axons that would normally project to the CC are redirected to the internal capsule in the *Unc5C* mutant. We performed similar DiI retrograde-labelling experiments in *Unc5C*$^{-/-}$ brains and counted the number of Satb2-positive cells projecting to the internal capsule (Fig. 5c,d). We found that the proportion of Satb2-positive, subcortically projecting cells was 16% higher in the *Unc5C* mutants compared with wild-type littermate brains (Fig. 5e; 49.1% in wild type versus 64.98% in *Unc5C*$^{-/-}$ brains, P-value = 0.0286, Student's t-test $n = 3$). Therefore, although callosal axons cross the midline in the *Unc5C* mutant, more Satb2-positive axons project to the internal capsule in both these mutants. This finding indicates that a Netrin1–Unc5C interaction plays an important role in determining the choice of axonal target projection (medially versus laterally), in a cell autonomous manner.

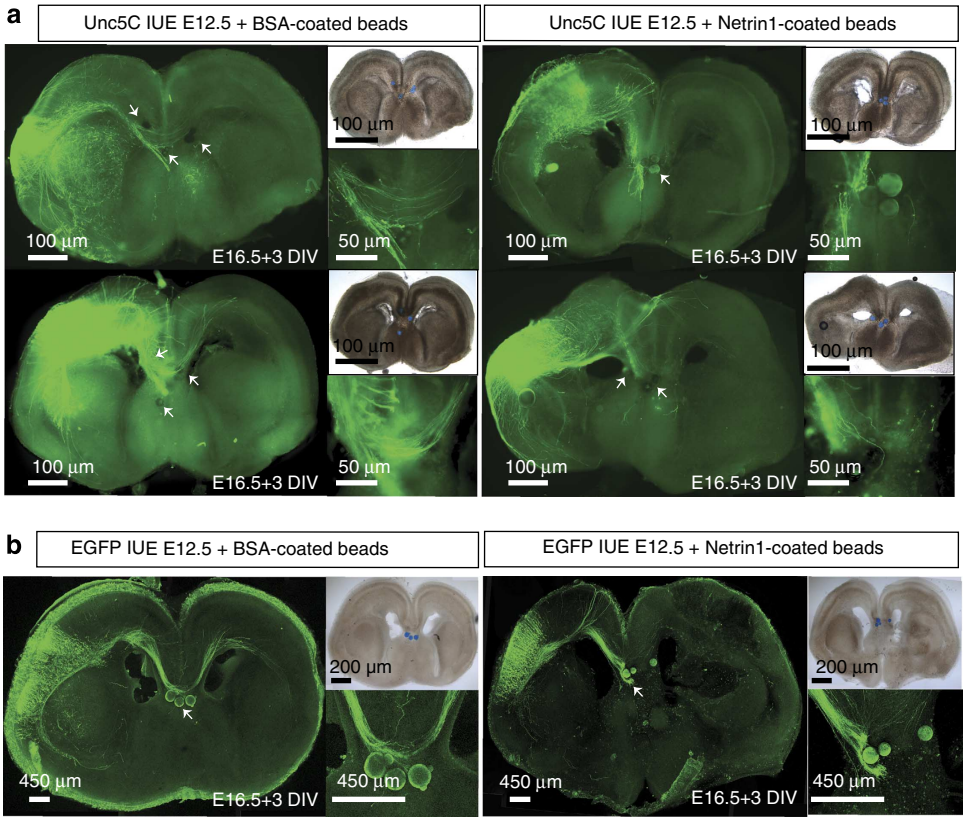

Figure 4 | Netrin1 repels Unc5C-positive neocortical axons. Images showing the axonal trajectory of neurons electroporated with *Unc5C* (**a**) or *EGFP* (**b**) on encountering neutral BSA-coated beads (arrows) or Netrin1-coated beads (arrows). Unc5C-positive fibres are unaffected by BSA-coated beads, placed along the midline, and continue along their initial trajectory to project into the contralateral hemisphere. Unc5C-positive fibres, upon encountering a Netrin1 source in the midline show clear repulsive behaviour with fibres projecting either dorsal or ventral to their initial path, but none continuing into the contralateral hemisphere. Wild-type axons electroporated with only *EGFP* (with endogenous Unc5C) are unaffected by the BSA beads and are repelled by the Netrin1 beads similar to the *Unc5C* overexpressing axons. Scale bar specified in the figure.

Satb2 is a direct repressor of *DCC* transcription. Since restoring the expression of *Unc5C* in *Satb2*$^{-/-}$ mutants lead to only a partial rescue of the CC, we tested whether additional axon guidance molecules in this pathway that are important in CC formation displayed altered expression in *Satb2*$^{-/-}$ brains. Like Unc5C, DCC is also a receptor for Netrin1, but has been shown to mediate axonal attraction[22]. We performed immunohistochemical staining and *in situ* hybridization for *DCC* in wild type as well as Satb2$^{-/-}$ cortices at E18.5. Both, DCC protein and mRNA expression was upregulated in Satb2$^{-/-}$ brains as compared with wild-type littermates (Fig. 6a). In contrast, no changes in *DCC* expression were observed between the control and Ctip2$^{-/-}$ or between the Satb2$^{-/-}$;Ctip2$^{-/-}$ double mutant and Satb2$^{-/-}$ single mutant indicating that Ctip2 did not effect *DCC* expression (Supplementary Fig. 7).

In the wild-type cortex, *DCC* demonstrated a very dynamic pattern of expression. In contrast to *Unc5C* expression, *DCC* mRNA expression is high in the cortical plate at E14.5 (Fig. 6b) and below detection levels at E18.5. Only a low level of DCC protein expression was observed in the white matter at E18.5 (Fig. 6a). In order to investigate if Satb2 could regulate *DCC* expression, we overexpressed *Satb2* and *Ski* prematurely in wild-type cortex at E11.5 and analysed the brains for *DCC* expression at E14.5. Again, *Ski* was co-electroporated to enable Satb2 to recruit the transcription repressor complex. At E14.5, since there are few endogenous Satb2-positive cells in the cortex and since *DCC* expression is high in the cortical plate, we assumed that any alteration in *DCC* expression would be observable. In this experiment, *DCC* expression was significantly lower in the electroporated region compared with the non-electroporated hemisphere ($n=2$). In contrast, *EGFP* electroporation alone did not alter the expression of *DCC* ($n=2$, Fig. 6b).

To investigate whether Satb2 could directly control *DCC* expression, we performed ChIP assays for two putative Satb2-binding sites (MAR1 and MAR2) upstream of the *DCC* transcription-initiation site (Fig. 6c). These regions are AT rich and could therefore serve as Satb2-binding sites. We observed a significant enrichment of the region more proximal to the TSS (MAR1) in wild-type tissue as compared with *Satb2*-mutant tissue, which served as the negative control (5.27 ± 2.75-fold enrichment in $n=6$ wild type compared with 1.72 ± 0.015 in $n=2$ *Satb2*$^{-/-}$ mutants, P-value $=0.025$, Student's t-test). In contrast, enrichment for the second MAR region (MAR2) was highly variable indicating that Satb2 might bind very weakly to this promoter region ($n=7$ wild type showed a range of 0.91–10.83-fold enrichment with an average of 4.69 ± 4.38, as compared with 1.47 ± 0.39 in $n=2$ *Satb2*$^{-/-}$ mutants, P-value $=0.10$, Student's t-test). To further investigate the functional significance of this MAR binding, we cloned the two genomic regions, *DCC* MAR1 and *DCC* MAR2, into a Gaussia Luciferase vector and transfected them into COS cells either in the presence or absence of *Satb2*. *DCC* MAR1 (chromosome 18 72356779–72357851) showed a 1.5-fold decrease in transcription levels when co-expressed with *Satb2* (Fig. 6d, $n=3$, P-value $=0.0035$, Student's t-test, $n=3$). *DCC* MAR2

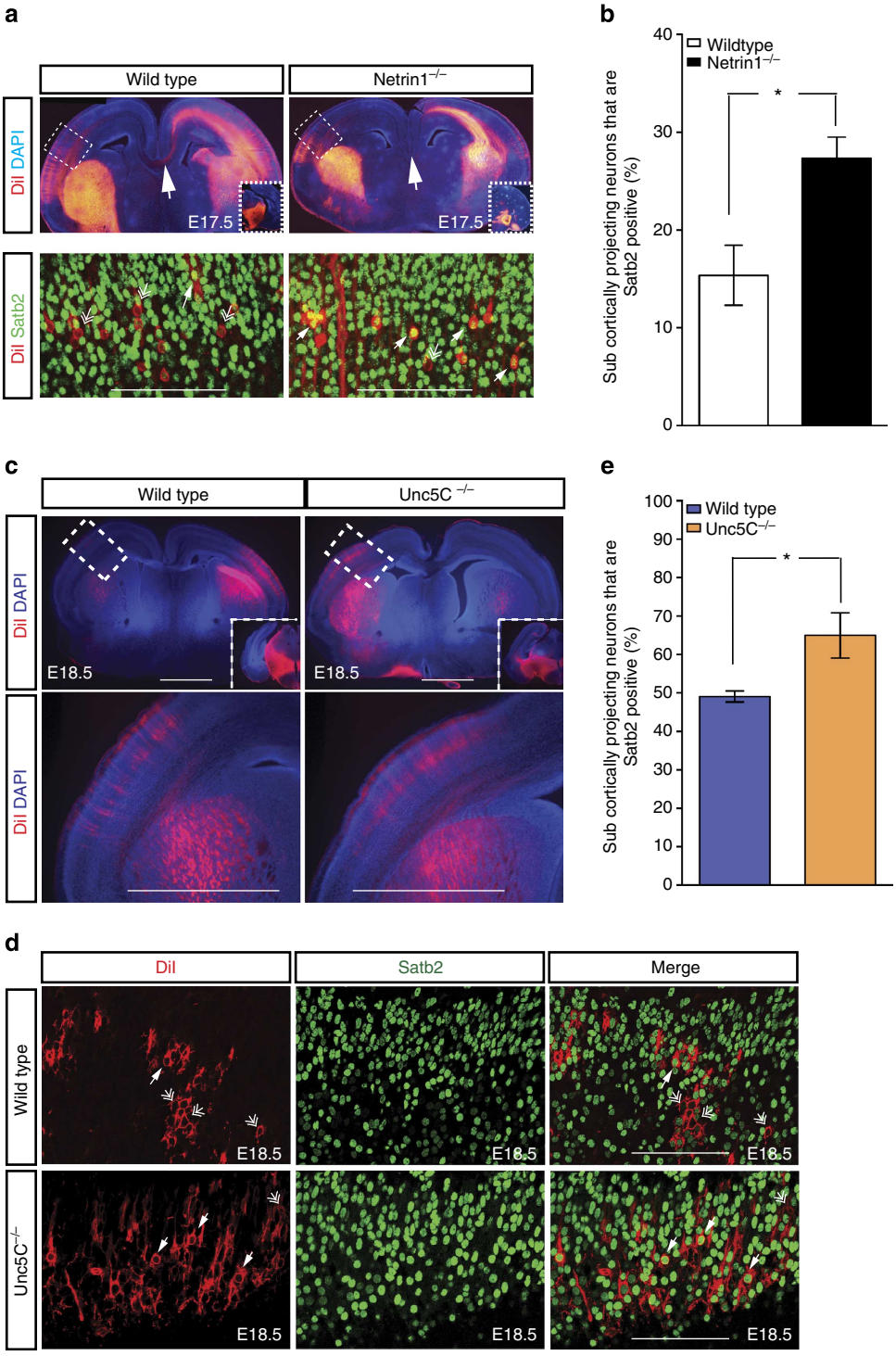

Figure 5 | Axons of Satb2 neurons are similarly misrouted to subcortical targets in *Netrin1* and *Unc5C*$^{-/-}$ mutants. (**a**) Retrograde labelling of subcerebrally projecting neurons by placing crystals of DiI in the cerebral peduncle of wild-type and *Netrin1*$^{-/-}$ brains. The smaller inset image shows the respective position of the crystal placement. Retrogradely labelled DiI-positive cells were colocalized with Satb2 in wild-type and *Netrin1*-mutant brains. Arrows point towards double-positive cells while double arrows highlight single DiI-positive cells. (**b**) Quantification of the percentage of DiI-positive cells that are Satb2 positive; 15.36% in wild type versus 27.33% in E17.5 *Netrin1* mutant, *P-value = 0.011 (Student's t-test), $n = 3$. Error bars represent s.e.m. (**c**) Crystals of the lipophilic tracer DiI were placed in the cerebral peduncle of wild-type and *Unc5C*$^{-/-}$ brains to retrogradely label cortical neurons projecting subcerebrally. The smaller inset images show the location of the crystals placed in the cerebral peduncle. Higher magnification image of the boxed region show layer V neurons back-labelled in the cortex. (**d**) Colocalization of DiI-positive and Satb2-positive cells in the neocortex. Arrows indicate double-positive cells, while double arrows indicate single DiI-positive cells. Scale bar, 100 μm. (**e**) Quantification of the proportion of subcortically projecting neurons that are Satb2 positive; 49.10% in wild type versus 64.98% in E18.5 *Unc5C*$^{-/-}$; *P-value = 0.0286 (Student's t-test), $n = 3$. Error bars represent s.e.m.

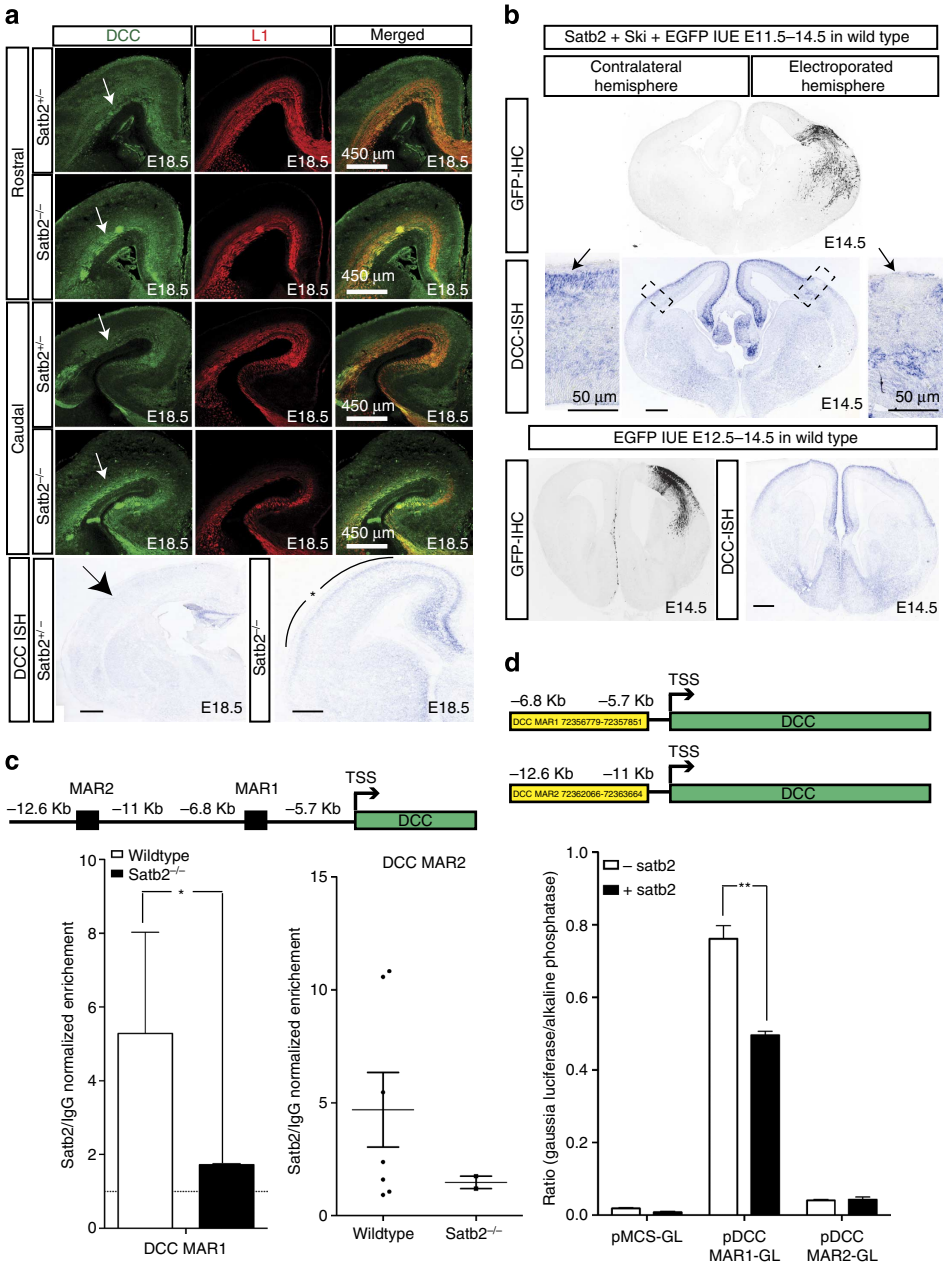

Figure 6 | *DCC* is negatively regulated by Satb2 and is upregulated in the *Satb2*$^{-/-}$ cortex. (**a**) Immunohistochemical staining for DCC in rostral and caudal sections shows an upregulation of DCC expression in *Satb2*$^{-/-}$ mutant brains as compared with wild-type littermates. Arrows point to the region of altered DCC expression between wild-type and *Satb2*$^{-/-}$ sections. ISH reflects an upregulation of *DCC* in E18.5 *Satb2*$^{-/-}$ cortex when compared with *Satb2* heterozygous brains. (**b**) Series of images show *DCC* expression in E14.5 wild-type embryos in cells electroporated with either *Satb2/Ski/EGFP* at E11.5 or with *EGFP* alone at E12.5. GFP IHC delineates the region electroporated. *DCC* ISH demonstrates a downregulation of *DCC* mRNA within cells electroporated with *Satb2/Ski* compared with *DCC* expression in the contralateral hemisphere, or in the control electroporation. (**c**) Schematic diagram showing two putative binding MAR sites for Satb2 upstream of the *DCC* transcription-initiation site. ChIP from P0 cortices showed a 5.27 ± 2.75-fold enrichment in $n = 6$ wild-type compared with 1.72 ± 0.015 in $n = 2$ *Satb2*$^{-/-}$ mutants for *DCC* MAR1, **P*-value = 0.025 (Student's *t*-test) and for *DCC* MAR2, $n = 7$ wild-type showed a range of 0.91–10.83-fold enrichment with an average of 4.69 ± 4.38, as compared with 1.47 ± 0.39 in $n = 2$ *Satb2*$^{-/-}$ mutants, *P*-value = 0.10 (Student's *t*-test). (**d**) Luciferase assay to demonstrate that Satb2 binds to the *DCC* genomic region and represses its expression. In the presence of full-length *Satb2*, *DCC* MAR1 showed a 1.5-fold decrease in luminescence ratio while *DCC* MAR2 did not shown any change (Student's *t*-test, ***P*-value = 0.0035). Scale bar, 100 µm, unless specified differently in the figure.

(chromosome 18 72362066–72363664) did not show any change in transcription levels upon *Satb2* co-expression (Fig. 6d, $n = 3$, *P*-value = 0.742, Student's *t*-test, $n = 3$). Taken together, these findings suggest that Satb2 can directly repress *DCC* expression and might be another factor influencing corticocortical versus cortico-subcortical axon targeting choice.

Downregulating DCC in Satb2$^{-/-}$ **partially rescues the CC.** To test the hypothesis that *DCC* upregulation contributed to the misrouting of callosal axons in Satb2-deficient brains, we tested whether downregulating *DCC* in the *Satb2* mutant could restore callosal projections. We tested the downregulation efficiency of four different small hairpin RNA (shRNA) constructs by

transfecting *DCC* shRNA or the scrambled shRNA together with a *DCC* expression plasmid in HEK cells and checking protein levels by western blot (Supplementary Fig. 8). Based on these experiments, we selected two *DCC* shRNA constructs (clone 2 and 4) and co-electroporated them with *Venus-GFP* at E12.5 in *Satb2*$^{-/-}$ and wild-type cortices. While callosal axons crossed the midline in wild-type brains electroporated with either the *DCC* shRNA or the scrambled shRNA, no midline crossing fibres were observed when scrambled shRNA was electroporated in *Satb2*$^{-/-}$ brains ($n=2$). In contrast, neurons electroporated with *DCC* shRNA in the *Satb2*$^{-/-}$ cortex now extended towards and crossed the midline ($n=3$, Fig. 7, Supplementary Fig. 3). The rescue was, however, again only partial.

Together, these results indicate that Satb2 directly represses the expression of *DCC* and that an upregulation of *DCC* in the *Satb2*$^{-/-}$ cortex could contribute to the lack of callosal axons crossing the midline. It is also interesting to note that downregulation of *DCC* at later stages of development (E14.5), could not restore callosal projections, indicating that only a population of deep layer neurons contributed to forming the restored projections (Supplementary Fig. 6B). In order to test whether the extent of CC restoration in *Satb2* mutants could be enhanced, we simultaneously inactivated *DCC* and overexpressed *Unc5C* in *Satb2* mutants. Surprisingly, in these experiments, we did not detect any CC restoration (Supplementary Fig. 9).

Satb2/Ctip2 control of DCC/Unc5C regulates only DL callosal projections. Callosal neurons are a heterogeneous population of neurons[23]. With respect to the molecular mechanisms described here, deep neocortical layers, born before E14.5 are dependent upon the Netrin1/Unc5C/DCC pathway. However, upper layer neurons, born after E14.5 probably require pathway(s) other than Netrin1/Unc5C/DCC. The lack of a complete restoration of the CC in *Satb2* mutants after *Unc5C* upregulation or *DCC* downregulation, questioned the extent of the cell autonomous contribution of *Satb2* to CC formation. We therefore electroporated a *Satb2* expression plasmid together with *EGFP* into *Satb2*$^{-/-}$ brains at E12.5. At E18.5, we observed that although the electroporated neurons in the *Satb2*$^{-/-}$ mutants were able to form a CC, the rescue of the CC was again only partial, similar to the rescues obtained in case of either the *Satb2*$^{-/-}$;*Ctip2*$^{-/-}$ double mutants, *Unc5C* overexpression or *DCC* downregulation in the *Satb2*$^{-/-}$ mutants ($n=2$, Fig. 8, Supplementary Fig. 3). A similar principal seems to be underlying all of these scenarios as *Satb2* upon ectopic overexpression in wild-type cortices can lead to *Unc5C* overexpression (Fig. 1b) and *DCC* downregulation (Fig. 6b). We also tested the ability of the electroporated *Satb2* in repressing *Ctip2* and found an absence of Ctip2 protein from the electroporated cells (Supplementary Fig. 10).

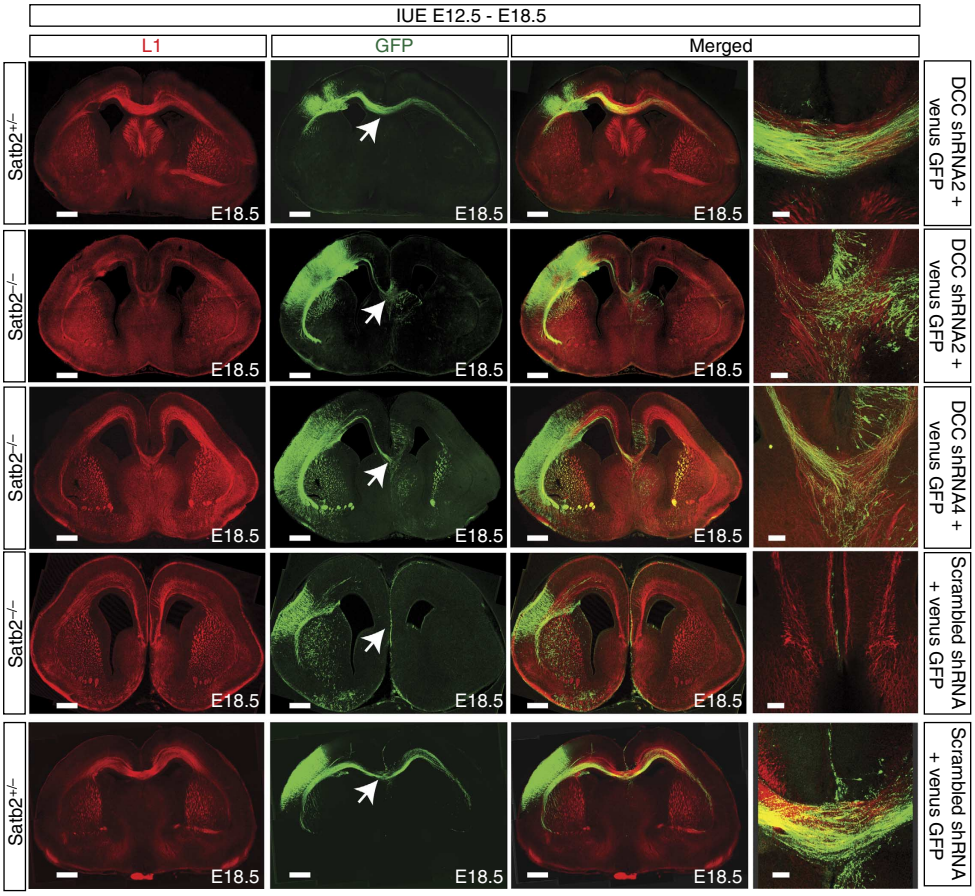

Figure 7 | Downregulating *DCC* in the *Satb2*$^{-/-}$ cortex leads to a partial rescue of the CC. Images show a series of experiments, wherein *in utero* electroporation was done at E12.5 and the brains harvested and analysed at E18.5. *In utero* electroporation of *DCC* shRNA and *Venus-GFP* do not seem to have a major effect on the formation of the CC in wild-type embryos. *In utero* electroporation of two different *DCC* shRNAs (shRNA2 and shRNA4) along with *Venus-GFP* shows a reproducible partial rescue of the CC in *Satb2*$^{-/-}$ embryos. *In utero* electroporation of a scrambled shRNA and *Venus-GFP* cannot rescue the CC in *Satb2*$^{-/-}$ embryos. Arrows point towards the dorsal midline. Scale bar, 450 μm for low-magnification images and 100 μm for high-magnification images.

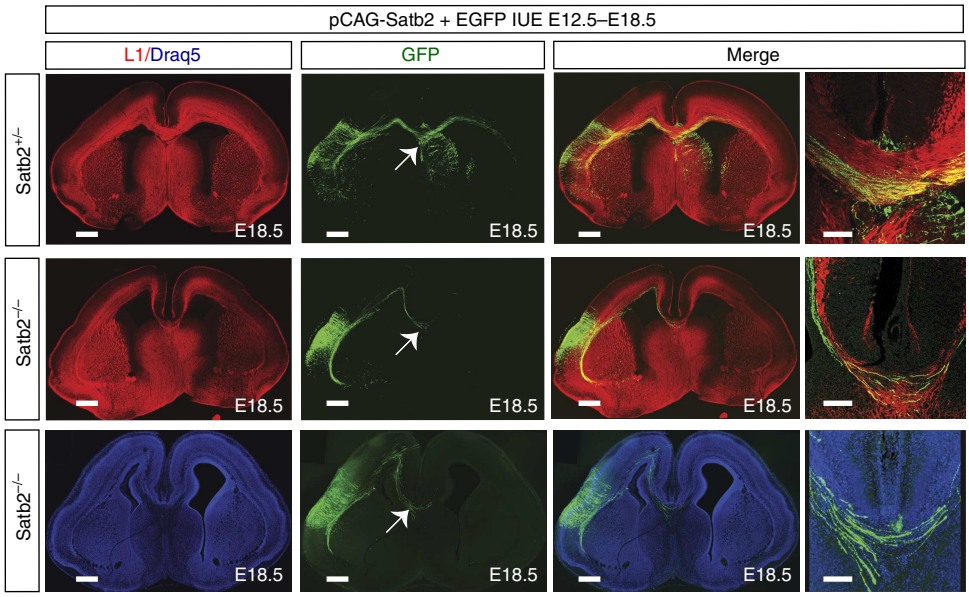

Figure 8 | *Satb2* electroporation in *Satb2*$^{-/-}$ cortex partially rescues the CC. *In utero* electroporation of plasmids encoding for *Satb2* and *EGFP* in wild-type and *Satb2*$^{-/-}$ embryos at E12.5, harvested at E18.5 followed by immunohistochemical staining for the neuronal adhesion molecule L1, show a partial rescue of the CC in *Satb2*$^{-/-}$ mutants. Alternatively, sections were counter stained with the far-red nuclear marker Draq5. Arrows indicate fibres crossing the midline. Scale bar, 450 μm for low-magnification images and 100 μm for high-magnification images.

Again, we did not observe any rescue of the CC upon overexpression of *Satb2* at later stages (E14.5, Supplementary Fig. 6C).

Discussion

The information processing ability of the nervous system relies heavily on the precise establishment of neuronal connections. The expression of *Satb2* or *Ctip2* in cortical neurons confers mutually exclusive genetic programs with respect to their targeting[7,8,24]. *Ctip2* dictates a corticofugal fate and is required for the fasciculation and appropriate targeting of these fibres[6]. In contrast, deletion of *Satb2* from the neocortex results in the absence of the CC, misrouting of callosal axons towards the internal capsule and an ectopic upregulation of *Ctip2* in callosal neurons[7,8]. It is interesting to note that although callosal axons fail to cross the midline in *Satb2* mutants, not all callosal neurons express *Satb2* (ref. 8). This suggests that callosal axons may require Satb2 both cell intrinsically and extrinsically. At the same time, some Satb2-positive neurons in deep cortical layers, do not downregulate *Ctip2*, and project to the internal capsule[8]. Satb2 was shown to require the transcriptional cofactor Ski in order to repress *Ctip2*; therefore, these Satb2-positive/Ctip2-positive/Ski-negative cells are most likely non-callosal neurons[20].

Data presented here indicate that ectopic upregulation of *Ctip2* in callosal neurons is one of the reasons that contribute to the lack of a CC in *Satb2*$^{-/-}$ mutants as upon deletion of *Ctip2* from the *Satb2*$^{-/-}$ cortex, the CC was partially restored. Similar results were also recently reported[7,19]. Since the upregulation of *Ctip2* in *Satb2*$^{-/-}$ mutants is a cell intrinsic effect, the rescue we observed in the *Satb2*$^{-/-}$; *Ctip2*$^{-/-}$ brains is likely to reveal the cell autonomous ability of *Satb2*-positive neurons to form the CC[8]. Unc5C and DCC act as receptors for the secreted ligand Netrin1, mediating either a chemorepulsive (Unc5C-DCC together) or a chemoattractive (DCC alone) response[22,25–27]. The expression of these two genes is differentially regulated in the neocortex of Satb2 mutants: while *Unc5C* level is down, *DCC* is upregulated (Fig. 9d).

We observed that Unc5C expression is regained in Satb2$^{-/-}$Ctip2$^{-/-}$ compound mutants and that Ctip2 acts as a direct transcriptional repressor of *Unc5C*. Overexpression of *Unc5C* in *Satb2*$^{-/-}$ mutants also leads to a partial restoration of the CC, demonstrating a cell autonomous ability for *Unc5C* to promote callosal targeting[28]. Srinivasan *et al.*[19], independently confirmed this result in a recent publication[7]. This finding at the outset raises the question: If *Unc5C* is required for CC formation then why are there no obvious defects of the CC observed in *Unc5C*$^{-/-}$ mutants? Retrograde labelling of subcortically projecting neurons in *Unc5C*$^{-/-}$ mutants showed that these mutants display an increase in the number of Satb2-positive neurons that project subcortically in these brains (Fig. 9f). This indicates that *Unc5C* is probably required for CC formation only in those neurons that rely on *Satb2* cell intrinsically to project callosally. These neurons seem to be early born deep layer neurons but not later born upper layer neurons. Since these axons comprise a smaller population of the CC it is possible that the misrouting of these axons is not easily detected in *Unc5C* mutants.

Unc5C-mediated CC formation is dependent on Unc5C-Netrin1 repulsion. We showed that similar to the *Unc5C* mutants, *Netrin1* mutants had a higher proportion of Satb2-positive cells projecting subcortically compared with wild-type brains. The differences in the proportion of Satb2-positive cells that we observed projecting subcortically in *Unc5C*$^{-/-}$ when compared with *Netrin1* mutants might be due to the different genetic backgrounds of these strains and/or because of the involvement of other Netrin1 receptors such as DCC and Draxin[29,30]. It is interesting to note that the *Netrin1* mutant is acallosal where as the *Unc5C* mutant is not. A probable explanation for this could be that although *Netrin1* mutants lack a CC, the majority of callosal fibres none the less arrive at the midline but are unable to cross, forming Probst bundles instead[31]. This could be due to the absence of midline Netrin1 expression that otherwise attract DCC expressing cingulate axons, forming the pioneer axons of the CC (Fig. 9a,e)[32]. However, in *Unc5C* mutants, since the midline Netrin1 interaction with DCC-positive cingulate axons is not

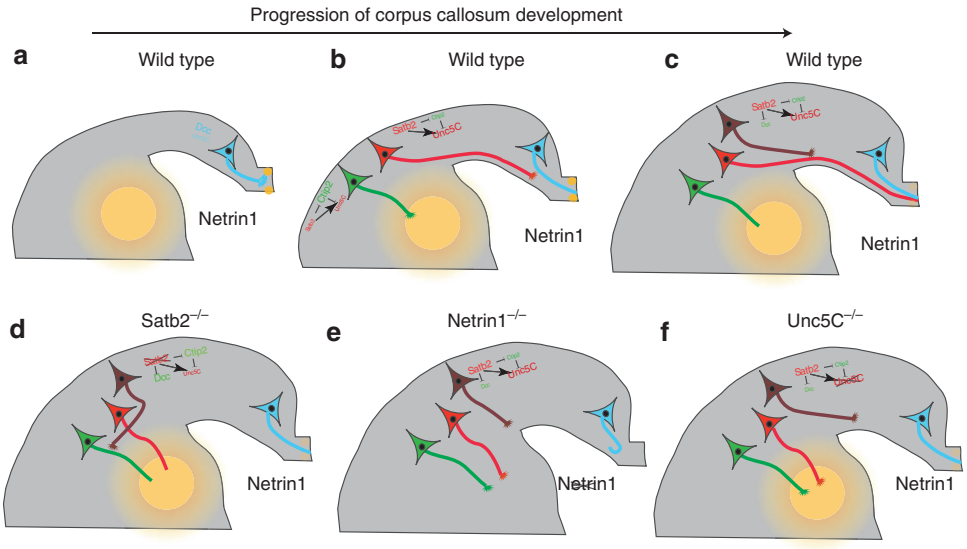

Figure 9 | *Satb2*- and *Ctip2*-dependent establishment of cortical connections. (**a**) During early corticogenesis, cingulate neurons with high DCC expression form the pioneer axons for the CC. These axons respond to midline Netrin1 and are attracted towards the Netrin1 source. (**b**) Later, when Layer V cells start projecting medially, Satb2 represses *Ctip2*, thereby promoting *Unc5C* expression. These Unc5C axons are repelled by the Netrin1 source in the internal capsule and thus turn towards the midline. Corticofugally projecting neurons, however, express high Ctip2 and thus repress *Unc5C*. In addition, the lack of repression of *DCC* by Satb2, promotes high DCC levels in these neurons. Thus, these axons are attracted towards the internal capsule (**c**). Despite expressing high levels of Unc5C and low levels of DCC, upper layer neurons are not dependent on these molecules and instead either follow the deep layer callosal pioneer axons or are dependent on other axon guidance molecules. (**d**–**f**) Represent the scenario in the *Satb2*, *Netrin1* or *Unc5C* mutants, respectively. In each of the mutants, the lack of an Unc5C-Netrin1 interaction causes a misrouting of deep layer callosal axons to subcortical targets.

disrupted, callosal axons cross the midline. Therefore, our data suggest that in *Netrin1* mutant and *Unc5C*$^{-/-}$-mutant mice, only the callosal fibres that depend on Netrin1–Unc5C interaction, misproject to subcortical targets, whereas neurons that depend on other signalling pathways, continue to project medially towards the midline, where in the *Unc5C*$^{-/-}$ brains they cross the midline but in the *Netrin1*-mutant brains they stall at the midline (Supplementary Table 1). Further, *Unc5C*-expressing cortical neurons are not repelled by midline Netrin1 probably because at late embryonic stages (E16.5 onwards) the expression level of Netrin1 in the midline is very low as compared with the expression in the basal ganglia[21,32] and axons of later born neurons do not require midline Netrin1 to form the CC[32].

In addition, we observed that *DCC* was upregulated in the absence of *Satb2* (Fig. 9d). We hypothesized that due to DCC-Netrin1 attraction and the absence of Unc5C-Netrin1-mediated repulsion in *Satb2* mutants, callosal fibres that are normally repelled by Netrin1 in the internal capsule are now attracted and hence project subcortically. Interestingly, we found that downregulation of *DCC* by electroporation of *DCC* shRNA in *Satb2*$^{-/-}$ mice, resulted in a partial rescue of the CC while the *DCC* mutant displays an acallosal phenotype[22]. This apparent discrepancy could probably again be explained by the fact that although the *DCC* mutant lacks a CC, cortical axons navigate towards the midline but fail to cross the midline, forming Probst bundles instead[22]. As *DCC*-positive cingulate axons act as pioneers for the CC, the lack of neocortical callosal midline crossing in *DCC* knockout animals therefore appears to be due to a secondary defect.

In contrast to both the *Netrin1* and *DCC* mutant, in the *Satb2* mutant, the acallosal phenotype is not restricted to the absence of callosal midline crossing, but occurs because of the absence of any neocortical axons navigating medially (Supplementary Table 1). *Satb2* mutants do not display Probst bundles. All the axons are routed towards the internal capsule and anterior commissure[7,8]. Overexpression of *Unc5C* or downregulation of *DCC*, in *Satb2*$^{-/-}$ brains results in a subset of neurons projecting medially, which can be seen as a clear bundle of axons leaving the electroporated region and approaching the midline. Hence it is not just the midline crossing of these axons that is significant, but more so the choice to project interhemispherically and not in the corticofugal direction. Although we have not been able to detect any neocortical axons forming the CC in our *Satb2* mutant, Alcamo *et al.*[7] reported that their *Satb2* mutant has a severely reduced callosum. These few fibres that remain in the *Satb2* mutant could be attributed to the presence of *DCC*-positive cingulate axons that project interhemispherically through the CC that maybe unaffected in the *Satb2* mutant (Fig. 9d).

A simultaneous co-electroporation of *Unc5C* together with *DCC* shRNA did not result in a more profound rescue of the CC. Instead, we observed that there was no rescue at all. This is a surprising result indicating that the dosage of Unc5C/DCC in each cell might be critical in deciding the projection fate of cortical projection neurons[33].

Therefore, together, these experiments indicate an important role for *Netrin1*, *DCC* and *Unc5C* interaction in the trajectory choice made by deep layer cortical axons. We suggest a scenario where the source of Netrin1 in the internal capsule attracts Unc5C-negative/DCC-positive axons while repelling Unc5C-positive/DCC-negative axons. Hence, callosally projecting deep layer neurons require higher levels of Unc5C and lower levels of DCC while on the other hand, low levels of Unc5C and high levels of DCC instruct neurons to project subcortically. It is still not clear how this Netrin1-DCC/Unc5C interaction mechanism functions during the initial steps of axon navigation. We suggest two alternative scenarios. One possibility is that cortical neurons send two axonal branches in two opposite directions, one towards CC and the other towards the internal capsule. The presence of such dual projections in early neocortical development has been reported previously[24,34]. Here, Unc5C-positive/DCC-negative

neurons would retract the lateral branch after arrival at the Netrin1 source in the internal capsule and stabilize the callosal branch. Unc5C-negative/DCC-positive neurons would retract the callosal branch and stabilize their subcortical branch. A second alternative scenario is that all early cortical neurons send their axons towards the internal capsule, but upon reaching the vicinity of a Netrin1 source, Unc5C-positive/DCC-negative neurons would retract these axons and develop an independent callosal branch. Further studies using live cell imaging would be required to address this issue.

Our data strongly indicates that the control of *Satb2* and *Ctip2* over callosal and corticofugal fate specification is dependent on *Unc5C* and *DCC* only with respect to deep layer neurons as none of the rescue experiments performed at E14.5 lead to the formation of a CC. Second, the DiI experiments on *Unc5C* and *Netrin1* mutants predominantly labelled deep layer neurons and thus the differences that we report here are most likely a reflection of the misrouting of deep layer Satb2-positive neurons. Electroporation of *Satb2* into the *Satb2*$^{-/-}$ brain could as well not rescue the entire acallosal phenotype in these mice, and was effective in rescuing only early born, deep layer, callosal projections. This clearly shows that the potential of each individual Satb2-positive cell to project callosally is highly limited and requires a supportive environment. Hence, it is likely that deep layer neurons act in a cell autonomous manner in deciding between callosal and subcortical fates and that later born Satb2-positive cells are dependent on other mechanisms for correct path finding.

Methods

Mouse mutants. All mouse experiments were carried out in compliance with German law and were approved by the Bezirksregierung Braunschweig and the University of Queensland animal ethics committee. The *Satb2-*, *Ctip2-*, *Unc5C-* and *Netrin-1*-mutant mice were generated as described previously[12,13,35,36]. The day of vaginal plug was considered embryonic day (E) 0.5. Wild-type mice used were from a NMRI background. Both male and female embryos were used for the study.

Data analysis. Data was analysed using Excel or GraphPad Prism. Student's *t*-test was used for determining statistical significance.

Outgrowth assay. *Satb2Cre;Rosa flox stop lacZ* mice were time-mated (E13 or E17) and pregnant dams were anesthetized with 100 mg kg^{-1} sodium pentobarbitone, and placed on a heating pad. Embryos were removed and placed in Leibovitz's L-15 medium (Invitrogen), the brain was removed, and the neocortex dissected. Explants and collagen gels were prepared and cultured exactly as described earlier[32]. Explants displaying poor growth (those below one standard deviation (s.d.) of the mean level of outgrowth for all experiments across all conditions) were eliminated from the experiment. Each explant was stained with TuJ1 IHC as previously described[32] and imaged using a Zeiss upright microscope equipped with an Apotome optical sectioning device. Digital images were analysed using a Matlab (The Mathworks) programme to define a line through the centre of the explant (centre of mass of pixels representing the explant body). The number of pixels representing neurites on either side of this line was then counted (values U and D, respectively). 'Outgrowth' was defined as total neurite pixels (U + D) divided by the total number of pixels representing the neurite body[37,38]. A total of 46–139 explants per condition were pooled across four experiments and the amount of outgrowth analysed using an unpaired two-tailed Student's *t*-test. Data are presented as average values ± standard error of the mean (s.e.m.).

Tissue processing and IHC. Brains were dissected and washed in ice-cold phosphate-buffered saline (PBS) and fixed overnight with 4% paraformaldehyde (wt/vol) followed by treatment with cryo-preservant sucrose and embedding in TissueTek or were processed for vibratome sectioning by embedding in 4% agarose (Applichem). Accordingly, (10 m thick coronal were cut on a cryostat or 80 µm thick on a vibratome. All sections were blocked for 1 h at 24 °C with a solution of 0.1% Triton X-100 (vol/vol) and 2% BSA (wt/vol) in PBS. This was followed by application of the primary antibodies. All antibodies were incubated overnight at 4 °C. Alexa (Molecular Probes) or Dylight (Jackson Immunoresearch) Fluor–tagged secondary antibodies were used at a dilution of 1:500 for 1 h at 24 °C. All sections were mounted in fluorescent mounting medium (DakoCytomation, s3023). The blocking solution used for DiI-labelled sections was 2% BSA in PBS and did not contain any detergent.

Primary antibodies used for IHC. We used antibodies against GFP (goat, Rockland, 600-202-215, 1:500), Ctip2 (rat, Abcam, ab18465 1:200), DCC (1:100, a kind gift from Dr Helen Cooper), Unc5C (rabbit, self-generated, 1:300), Satb2 (rabbit, self-generated, 1:1,000), L1 (rat, Millipore, MAB5272, 1:150), Calretinin (rabbit, 1:1,000, Swant) and glial fibrillary acidic protein (mouse, 1:500, Sigma).

DiI labelling and quantification. After fixation in 4% PFA (*Unc5C*-mutant brains used for the labelling were fixed for 8 h while the *Netrin1*-mutant brains used for the labelling were fixed for more than 3 years), single crystals of 1,1′-dioctadecyl-3,3,3′,3′-tetramethylindocarbocyanine perchlorate (DiI, Molecular probes) were placed with a stainless steel electrode into the cerebral peduncle of the brains. After DiI placement, brains were kept for 2 weeks at 37 °C in PBS with 0.1% sodium azide in the dark. After incubation for the stipulated time, brains were embedded in 4% agarose and sectioned into 80-µm thick sections using a vibratome. Sections were counterstained with Hoechst (Sigma) and mounted in PBS. Alernatively, sections were processed for immunostaining with Satb2. No detergent was used for staining DiI-labelled sections. Images were procured on a Leica SL/SP2 confocal microscope and counting was done manually. Statistics was done using R and Microsoft excel. Graphs were made on GraphPad prism 5. Data are presented as average values ± s.d.

***In Utero* electroporation.** This procedure was carried out as described before[39]. Briefly, pregnant females were anesthetized using Isoflurane inhalation. Temgesic was administered subcutaneously as a painkiller. A 30-mm incision was made into the skin and then the abdominal wall along the midline. Carefully, embryos from either side of the uterine wall were pulled out. Embryos were continuously bathed with a warm solution of 1 × PBS supplemented with penicillin (1,000 units ml^{-1})–streptomycin (1,000 µg ml^{-1}) to minimize chances of infection. The plasmid solution was injected into one or both lateral ventricles with the help of a picospritzer. Electroporation was carried out by applying six electric pulses of 35 V each, 50 ms duration and 950 ms interval. The animals were allowed to recover and then returned to their cage and kept under observation. At the stage of harvest, the brains were isolated and checked for fluorescence. The brains were then fixed in 4% PFA overnight and embedded in 4% agarose (Applichem) for sectioning using a vibratome. Data are presented as average values ± s.e.m.

Plasmids. The *Unc5C, Satb2, and Ski* overexpression plasmids were a kind gift from Dr Frank Polleux, Dr Nenad Sestan and Dr Suzana Atanasoski, respectively. Dr Handjantonakis and Dr Leid kindly provided the CAG-venus-GFP and the pCMV-Ctip2 overexpression plasmid, respectively. The pCAG-Ctip2 overexpression plasmid was cloned by polymerase chain reaction (PCR) from first strand mouse E17.5 cDNA and inserted into the EcoR1-Not1 sites of pCAG. The insert was verified by sequencing. The DCC shRNAs used were purchased from GeneCopoeia. The four different target sequences used were aagccggatgaaggacttt (*DCC* shRNA1), agagaccatccaacgtaat (*DCC* shRNA2), ttgtcgcctacaatgagtg (*DCC* shRNA3), agcagcggtactattccat (*DCC* shRNA4). Scrambled shRNA with an unrelated RNA sequence was used.

The following primers were used for cloning the *Unc5C* and *DCC* RNA probes:
Unc5C1 fwd 5′-TCGAATTCGCCGCCACCATGAGGAAAGGTCTGAGGGC GACAG-3′
Unc5C1 rev 5′-AGAGAGTTGAAGGTACCAAATGCTGTGCA-3′
Unc5C2 fwd 5′-TGCACAGCATTTGGTACCTTCAACTCTCT-3′
Unc5C2 rev 5′-TACCCGGGAATACTGTCCTTCTGCTGCCAAGGA-3′
DCC fwd 5′-CCCGATCTTTGGATACATCATGAAG-3′
DCC rev 5′-TCAAAAGGCAGACCCTGTGATGGCGTT-3′.

The PCR products were cloned into pGEMT (Promega) and transcribed with T7/Sp6 promoters to generate the RNA probes.

***In situ* hybridization and combined IF-FISH.** Chromogenic *in situ* hybridization was performed on overnight fixed tissue samples. Tissues were sectioned with a cryostat at 14–16 µm thickness. Subsequently, the tissue was post-fixed for 15 min in 4% PFA, followed by two PBS washes. The tissue was then treated with Proteinase K for 3 min at room temperature in order to permeabilize the tissue. This step was omitted for the IF-FISH protocol and was instead substituted with a 25-minute incubation in 2 × SSC pH 7.0 (ref. 40). Following this, the tissue was either washed in PBS with glycine (to stop the proteinase K reaction) or PBS (IF-FISH). The tissue was then pretreated with the pre-hybridization buffer (50% formamide, 5 × SSC pH 7.0, 2.5 M EDTA, 0.1% Tween-20, 0.15% CHAPS, 0.1 mg ml^{-1} Heparin, 100 µg ml^{-1} yeast tRNA, 50 µg ml^{-1} salmon sperm DNA, 1 × Denhardt's solution) for 2 h at 65 °C. Following this, the probe was applied and incubated overnight at 65 °C. The following day, the tissue was treated with RNaseA for 30 min at 37 °C, washed with 2 × SSC pH 4.5/50% formamide at 65 °C and then with KTBT (100 mM NaCl, 50 mM Tris–Hcl pH 7.5, 10 mM KCl, 1% Triton X-100). The tissue was then blocked in 20% sheep serum and then incubated overnight with sheep anti-DIG (Roche, 1:1,000) antibody. For the IF-FISH, antibodies against Satb2 and Ctip2 were also included. The following day, the tissue was washed in KTBT and NTMT (50 mM NaCl, 100 mM Tris–HCl pH 9.5, 50 mM $MgCl_2$, 0.5% Tween-20). The reaction was developed by adding substrate NBT/BCIP (Roche, chromogenic) or Fast Red (Abcam, IF-FISH). Upon

reaching the appropriate signal intensity, for the IF-FISH, the sections were washed in PBS and stained with appropriate secondary antibodies.

Slice culture and Bead implantation. We cut 200–250-μm thick sections of E16.5 *Unc5C* or *EGFP* electroporated brains using a vibratome and cultured them on cell culture inserts (1-ct pore size, BD Biosciences) according to the protocol described previously[41,42]. The slices were cultured in a medium consisting of complete Hank's Balanced Salt Solution, basal medium Eagle, 20 mM D-glucose, 1 mM L-glutamine, penicillin (100 U ml^{-1}), streptomycin (0.1 mg ml^{-1}), N2 supplement (100 μ, per 12.5 ml) and 10% heat-inactivated horse serum (vol/vol). Agarose beads (Affi-gel Blue gel, Bio-Rad Laboratories) were washed three times with sterile water and four times with PBS. For coating the beads with Netrin1, 20 μl of bead solution was mixed with 10 μl of a Netrin1 solution (250 ng μg^{-1} R&D Biosciences) and incubated overnight at 4 °C. BSA-coated beads were used as a control for which 20 μl of bead solution was mixed with 20 μl of BSA (1 mg ml^{-1}). Before placing the beads on the slices, they were washed with PBS and then resuspended in 100 μl. of slice culture medium. Using a mouth pipette, the beads of the desired size were picked and placed over the midline in the region where the CC crosses. The cultured slices were immunostained (see above) after 3 days.

Chromatin immunoprecipitation. The ChIP IT express kit (Active Motif) was used for performing the ChIP assay, according to the manufacturer's instructions. Rat monoclonal anti-Ctip2 (Abcam), Satb2 (self-generated) and polyclonal anti-rabbit IgG (Active Motif) antibodies were used. The following primers were used for quantitative real time polymerase chain reaction:

Unc5C E1 fwd: 5′-ATCAAGCGCAACTCCCTAAA-3′
Unc5C E1 rev: 5′-CTTGCTCACTTGCTCACTCG-3′
Unc5C E2 fwd: 5′-CCCTTGGAGAAAGTGGAGTG-3′
Unc5C E2 rev: 5′-GTGTACGGGGAAGGGAAAC-3′
DCC MAR1 fwd: 5′-TGCACAGCACCTATGATCTTG-3′
DCC MAR1 rev: 5′ AACAGAGGAGTCAGAGCGAAA-3′
DCC MAR2 fwd: 5′-CGCACACACATTATTCTTTTGG-3′
DCC MAR2 rev: 5′-ACTGCCTGGCTCTGTACTCC-3′.

Data are presented as average values ± s.d.

Luciferase Assay. The luciferase assay was done in HEK cells. *Unc5C* putative Ctip2-binding promoter regions were amplified with the following primers: E1Fw: 5′-TTAAGAATTCTTGCCTTCTTTCCCATCT-3′, E1Rv: 5′-TATTGAGGATCCAGTGCTGGGAGGTGTAGCGC-3′, E2Fw: 5′-TTAAGAATTCTCCTCCTCGGAGGCTC-3′, E2Rv: 5′-TATTGAGGATCCTGAGACGCGCAAACAGCCGA-3′.

The fragments were cloned into pC1-TK-luciferase vector (Evrogen). E1 and E2 fragments included −842 to −124 nt and −60 to +65 nt of the Unc5C 5′-flanking promoter region, respectively.

Lipofectamine 2000 (Invitrogen) was used for transfecting cells, according to the manufacturer's instructions. Transfected cells were analysed 24 h after transfection. Luciferase assays were done using the Dual-Luciferase kit (Promega). A mixture of plasmids coding for renilla luciferase (RL) were used (CMV-RL, TK-RL and SV40-RL; 1:2:10 molar proportions, respectively) to account for variable transfection efficiency. Lumat LB96V reader (Berthold Technologies) was used for reading the assays. Results are shown as Renilla-normalized relative luciferase units (RLUs) ± s.d. Data shown is at least from three independent experiments. All *P*-values were ≤ 0.05.

The following primers were used for cloning the DCC MAR1 and MAR2 regions. The PCR products were initially cloned into pGEMT (promega) and sequence verified. Subsequently, the MAR containing inserts were subcloned into pMCS-GL (Thermoscientific).

DCC MAR1 fwd 5′-ACTACCTAGTAGAGGCAGCCACAAG-3′
DCC MAR1 rev 5′-AGGTGAAATTTCCACCAATGTGAAT-3′
DCC MAR2 fwd 5′-AAAATGCTACCCATGTTCCAGAAG-3′
DCC MAR2 rev 5′-ACTGCCTGGCTCTGTACTCCAAATT-3′

Fragments cloned into pMCS-GL were transfected along with pCMV-alkaline phosphatase in COS cells using lipofectamine 2000. Forty-eight hours post transfection, cell media was collected and used for assaying using the secrete–Pair Dual Luminescence assay kit (Genecopoeia). Glomax (promega) was used for reading the plates. Values are represented as Ratio of Gaussia luciferase to alkaline phosphatase luminescence ratio ± s.d. Values were collected from three independent experiments, with at least three replicates for each experiment.

References

1. Richards, L. J., Koester, S. E., Tuttle, R. & O'Leary, D. D. Directed growth of early cortical axons is influenced by a chemoattractant released from an intermediate target. *J. Neurosci.* **17,** 2445–2458 (1997).
2. Kriegstein, A., Noctor, S. & Martinez-Cerdeno, V. Patterns of neural stem and progenitor cell division may underlie evolutionary cortical expansion. *Nat. Rev. Neurosci.* **7,** 883–890 (2006).
3. Marin-Padilla, M. Ontogenesis of the pyramidal cell of the mammalian neocortex and developmental cytoarchitectonics: a unifying theory. *J. Comp. Neurol.* **321,** 223–240 (1992).
4. Hill, R. S. & Walsh, C. A. Molecular insights into human brain evolution. *Nature* **437,** 64–67 (2005).
5. Richards, L. J., Plachez, C. & Ren, T. Mechanisms regulating the development of the corpus callosum and its agenesis in mouse and human. *Clin. Genet.* **66,** 276–289 (2004).
6. Arlotta, P. *et al.* Neuronal subtype-specific genes that control corticospinal motor neuron development *in vivo*. *Neuron* **45,** 207–221 (2005).
7. Alcamo, E. A. *et al.* Satb2 regulates callosal projection neuron identity in the developing cerebral cortex. *Neuron* **57,** 364–377 (2008).
8. Britanova, O. *et al.* Satb2 is a postmitotic determinant for upper-layer neuron specification in the neocortex. *Neuron* **57,** 378–392 (2008).
9. Szemes, M., Gyorgy, A., Paweletz, C., Dobi, A. & Agoston, D. V. Isolation and characterization of SATB2, a novel AT-rich DNA binding protein expressed in development- and cell-specific manner in the rat brain. *Neurochem. Res.* **31,** 237–246 (2006).
10. Kennedy, T. E., Serafini, T., de la Torre, J. R. & Tessier-Lavigne, M. Netrins are diffusible chemotropic factors for commissural axons in the embryonic spinal cord. *Cell* **78,** 425–435 (1994).
11. Keino-Masu, K. *et al.* Deleted in colorectal cancer (DCC) encodes a netrin receptor. *Cell* **87,** 175–185 (1996).
12. Serafini, T. *et al.* Netrin-1 is required for commissural axon guidance in the developing vertebrate nervous system. *Cell* **87,** 1001–1014 (1996).
13. Ackerman, S. L. *et al.* The mouse rostral cerebellar malformation gene encodes an UNC-5-like protein. *Nature* **386,** 838–842 (1997).
14. Metin, C., Deleglise, D., Serafini, T., Kennedy, T. E. & Tessier-Lavigne, M. A role for netrin-1 in the guidance of cortical efferents. *Development* **124,** 5063–5074 (1997).
15. Finger, J. H. *et al.* The netrin 1 receptors Unc5h3 and Dcc are necessary at multiple choice points for the guidance of corticospinal tract axons. *J. Neurosci.* **22,** 10346–10356 (2002).
16. Hong, K. *et al.* A ligand-gated association between cytoplasmic domains of UNC5 and DCC family receptors converts netrin-induced growth cone attraction to repulsion. *Cell* **97,** 927–941 (1999).
17. Su, M. *et al.* Regulation of the UNC-5 netrin receptor initiates the first reorientation of migrating distal tip cells in *Caenorhabditis elegans*. *Development* **127,** 585–594 (2000).
18. Gitai, Z., Yu, T. W., Lundquist, E. A., Tessier-Lavigne, M. & Bargmann, C. I. The netrin receptor UNC-40/DCC stimulates axon attraction and outgrowth through enabled and, in parallel, Rac and UNC-115/AbLIM. *Neuron* **37,** 53–65 (2003).
19. Srinivasan, K. *et al.* A network of genetic repression and derepression specifies projection fates in the developing neocortex. *Proc. Natl Acad. Sci. USA* **109,** 19071–19078 (2012).
20. Baranek, C. *et al.* Protooncogene Ski cooperates with the chromatin-remodeling factor Satb2 in specifying callosal neurons. *Proc. Natl Acad. Sci. USA* **109,** 3546–3551 (2012).
21. Barallobre, M. J. *et al.* Aberrant development of hippocampal circuits and altered neural activity in netrin 1-deficient mice. *Development* **127,** 4797–4810 (2000).
22. Fazeli, A. *et al.* Phenotype of mice lacking functional Deleted in colorectal cancer (Dcc) gene. *Nature* **386,** 796–804 (1997).
23. Molyneaux, B. J. *et al.* Novel subtype-specific genes identify distinct subpopulations of callosal projection neurons. *J. Neurosci.* **29,** 12343–12354 (2009).
24. Lickiss, T., Cheung, A. F., Hutchinson, C. E., Taylor, J. S. & Molnar, Z. Examining the relationship between early axon growth and transcription factor expression in the developing cerebral cortex. *J. Anat.* **220,** 201–211 (2012).
25. Hedgecock, E. M., Culotti, J. G. & Hall, D. H. The unc-5, unc-6, and unc-40 genes guide circumferential migrations of pioneer axons and mesodermal cells on the epidermis in *C. elegans*. *Neuron* **4,** 61–85 (1990).
26. Hamelin, M., Zhou, Y., Su, M. W., Scott, I. M. & Culotti, J. G. Expression of the UNC-5 guidance receptor in the touch neurons of *C. elegans* steers their axons dorsally. *Nature* **364,** 327–330 (1993).
27. Colamarino, S. A. & Tessier-Lavigne, M. The axonal chemoattractant netrin-1 is also a chemorepellent for trochlear motor axons. *Cell* **81,** 621–629 (1995).
28. Kim, D. & Ackerman, S. L. The UNC5C netrin receptor regulates dorsal guidance of mouse hindbrain axons. *J. Neurosci.* **31,** 2167–2179 (2011).
29. Islam, S. M. *et al.* Draxin, a repulsive guidance protein for spinal cord and forebrain commissures. *Science* **323,** 388–393 (2009).
30. Ahmed, G. *et al.* Draxin inhibits axonal outgrowth through the netrin receptor DCC. *J. Neurosci.* **31,** 14018–14023 (2011).
31. Ren, T., Zhang, J., Plachez, C., Mori, S. & Richards, L. J. Diffusion tensor magnetic resonance imaging and tract-tracing analysis of Probst bundle structure in Netrin1- and DCC-deficient mice. *J. Neurosci.* **27,** 10345–10349 (2007).
32. Fothergill, T. *et al.* Netrin-DCC signaling regulates corpus callosum formation through attraction of pioneering axons and by modulating Slit2-mediated repulsion. *Cereb. Cortex*. doi:10.1093/cercor/bhs395 (2013).

33. Muramatsu, R. *et al.* The ratio of 'deleted in colorectal cancer' to 'uncoordinated-5A' netrin-1 receptors on the growth cone regulates mossy fibre directionality. *Brain* **133,** 60–75 (2010).
34. Garcez, P. P. *et al.* Axons of callosal neurons bifurcate transiently at the white matter before consolidating an interhemispheric projection. *Eur. J. Neurosci.* **25,** 1384–1394 (2007).
35. Wakabayashi, Y. *et al.* Bcl11b is required for differentiation and survival of alphabeta T lymphocytes. *Nat. Immunol.* **4,** 533–539 (2003).
36. Britanova, O. *et al.* Satb2 haploinsufficiency phenocopies 2q32-q33 deletions, whereas loss suggests a fundamental role in the coordination of jaw development. *Am. J. Hum. Genet.* **79,** 668–678 (2006).
37. Rosoff, W. J., McAllister, R, Esrick, M. A., Goodhill, G. J. & Urbach, J. S. Generating controlled molecular gradients in 3D gels. *Biotechnol. Bioeng.* **91,** 754–759 (2005).
38. Mortimer, D. *et al.* Bayesian model predicts the response of axons to molecular gradients. *Proc. Natl Acad. Sci. USA* **106,** 10296–10301 (2009).
39. Saito, T. *In vivo* electroporation in the embryonic mouse central nervous system. *Nat. Protoc.* **1,** 1552–1558 (2006).
40. Nehme, B., Henry, M. & Mouginot, D. Combined fluorescent *in situ* hybridization and immunofluorescence: limiting factors and a substitution strategy for slide-mounted tissue sections. *J. Neurosci. Methods.* **196,** 281–288 (2011).
41. Polleux, F. & Ghosh, A. The slice overlay assay: a versatile tool to study the influence of extracellular signals on neuronal development. *Sci. STKE.* **2002,** pl9 (2002).
42. Seuntjens, E. *et al.* Sip1 regulates sequential fate decisions by feedback signaling from postmitotic neurons to progenitors. *Nat. Neurosci.* **12,** 1373–1380 (2009).

Acknowledgements

We would like to thank the following for generously sharing their materials and resources- Dr Kominami for the *Ctip2*-mutant mice, Dr Helen Cooper for the DCC antibody, Dr Franck Polleux for the CAG-Unc5C expression plasmid, Dr Handjantonakis for the CAG Venus-GFP plasmid, Dr Leid for providing the *Ctip2* expression plasmid used in luciferase assays, Dr Nenad Sestan for the *Satb2* overexpression plasmid and Dr Suzana Atanasoski for the pCAG-Ski plasmid. SP would like to thank Dr Zoltan Molnar for teaching the art of DiI tracing. The authors would also like to acknowledge the following for their contribution towards this work—Roman Wunderlich and Manuela Schwark for technical help, Paraskevi Sgourdou (former member V.T. lab) for pilot experiments and discussion and Steffen Schuster for help with western blot analysis. This work was supported by SFB665, DFG Heisenberg programme, DFG grant TA 303/3, Exzellenzcluster 257, National Health and Medical Research Council Australia, Project Grant 1043045 (L.J.R.), Max-Planck Society Fritz Thysson Foundation, Boehringer Ingelheim Fonds PhD Fellowships (S.S. and S.P.), Australian postgraduate award and Queensland Brain Institute top-up award (A-L.SD). L.J.R. is supported by a Principal Research Fellowship from the National health and Medical Research Council, Australia.

Author contributions

S.S., S.P., L.J.R. and V.T. designed the experiments. S.S., S.P., O.B., I.B. and A.-L.D. performed experiments. S.S., S.P., O.B., A.-L.D., L.J.R. and V.T. analysed the data. S.L.A. provided mouse mutants. S.S., S.P., L.J.R. and V.T. wrote and edited the manuscript. S.S. and S.P. contributed equally to the work.

Additional information

Supplementary Information accompanies this paper at http://www.nature.com/naturecommunications

Competing financial interests: The authors declare no competing financial interests.

Reprints and permission information is available online at http://npg.nature.com/reprintsandpermissions/

How to cite this article: Srivatsa, S. *et al.* Unc5C and DCC act downstream of Ctip2 and Satb2 and contribute to corpus callosum formation. *Nat. Commun.* 5:3708 doi: 10.1038/ncomms4708 (2014).